Hindawi
Mathematical Problems in Engineering
Volume 2021, Article ID 6642620, 14 pages
https://doi.org/10.1155/2021/6642620

Research Article

Optimization Design of Oil-Immersed Iron Core Reactor Based on the Particle Swarm Algorithm and Thermal Network Model

Fating Yuan,[1,2] **Kai Lv**,[1] **Bo Tang**,[1] **Yue Wang**,[1] **Wentao Yang**,[1] **Shihong Qin**,[3] **and Can Ding**[1]

[1]*College of Electrical Engineering & New Energy, China Three Gorges University, Yichang 443002, China*
[2]*Hubei Provincial Engineering Technology Research Center for Power Transmission Line, China Three Gorges University, Yichang 443002, China*
[3]*School of Electrical Engineering and Information, Wuhan Institute of Technology, Wuhan 430205, China*

Correspondence should be addressed to Fating Yuan; yuanfatinghss@163.com and Shihong Qin; qinsh798@163.com

Received 27 December 2020; Revised 12 January 2021; Accepted 22 January 2021; Published 17 February 2021

Academic Editor: Xiao-Shun Zhang

In this paper, according to the design parameters of oil-immersed iron core reactor, the thermal network model of windings is established by the thermo-electric analogy method, and the temperature distribution of the windings can be obtained. Meanwhile, a fluid-thermal coupled finite element model is established, the temperature and fluid velocity distribution are extracted, and the simulation results show that the error coefficient of temperature is less than 3% compared with the thermal network model, so the correctness of thermal network model has been verified. Taking the metal conductor usage and loss of windings as the optimization objects, the optimization method based on the particle swarm algorithm and thermal network model is proposed, and the Pareto optimal solutions between the metal conductor usage and loss of windings are given. The optimization results show that the metal conductor usage is reduced by 23.05%, and the loss is reduced by 20.25% compared with the initial design parameters, and the maximum temperature of winding does not exceed the expected value. Thus, the objects of low metal conductor usage and loss of windings are conflicted and cannot be optimized simultaneously; the optimization method has an important guiding significance for the design of oil-immersed iron core.

1. Introduction

The oil-immersed iron core reactor is an indispensable equipment in the power system, which plays the role of reactive power compensation, limiting the fault current and improving the power factor of the system [1]. However, the reactor encounters overheating and even burns out in the operation process, and the relevant studies show that the excessive temperature of the windings is the main reason [2]. The oil flow of the oil-immersed reactor enters the oil channels of the disc-type windings; the hot spot is formed as the convection heat dissipation capacity of each disc which is different; when the hot spot exceeds the limit, it will directly affect the safe and stable operation of the reactor. In order to reduce the temperature of reactor, the methods, such as increasing the cross-sectional area of conductor and oil channel width, are adopted; they can reduce the loss and temperature of the windings, but the metal conductor usage is increased. The loss and the metal conductor usage of windings are two key parameters in the design of reactor; in order to realize the low loss and the metal conductor usage simultaneously, the temperature calculation is needed and the optimization design method about the reactor is essential.

Currently, the relevant studies mainly include (1) the temperature calculation of the reactor. The finite-difference method is used to calculate the temperature of the reactor [3, 4], and it is merely suitable for the situations that the temperature and heat flux distribution of the coil surface are the same, which limits its practical application. The finite element model is adopted [5–7], and the detailed temperature and fluid velocity distribution of the reactor can be obtained, but the calculation process is complex and

calculation time is long. The thermal network model is put forward, and it was applied to the transformer windings [8]. On the basis, the optimization model of transformer windings is proposed [9–12]. In [13], the complex model of oil channels in windings is simplified to an approximate matrix of hydraulic channel, and the correctness has been verified. (2) The optimization design of the reactor. In [14], the finite element method is adopted to improve the heat dissipation efficiency of the windings by adjusting the oil channel width and the thickness of the coils, but the calculation time is large and the principle is not clear. In [15, 16], the thermal-electromagnetic combined optimization method is proposed to reduce the metal conductor, but the influence of air duct's width on the heat dissipation efficiency is not considered. In [17–21], the genetic algorithm and particle swarm optimization are applied to minimize the metal conductor usage or the loss of the transformer, but it can only realize the optimization of a single target, the overall optimization of the reactor cannot be achieved.

In this paper, taking the metal conductor usage and loss of windings as the optimization objects, the thermal network model of windings is established by the thermo-electric analogy method, the temperature distribution of the windings can be obtained, and the correctness has been verified by the fluid-thermal coupled finite element method. Meanwhile, the optimization method based on particle swarm algorithm and thermal network model is proposed, and the Pareto optimal solutions between the metal conductor usage and loss of windings are given. The optimization results show that the metal conductor usage is reduced by 23.05%, and the loss is reduced by 20.25% compared with the initial design parameters, and the maximum temperature of windings does not exceed the expected value, and the correctness has been verified.

2. The Structure and Equivalent Model of Windings

2.1. The Structure and Parameters of Core Reactor. The oil-immersed core reactor with a rated voltage of 26.4 kV and rated capacity of 66 MVA is selected as a research object. The disc-type windings are made of wires with insulating layer, which are surrounded on the iron core column. In the windings, the horizontal oil channels are formed between disc-type windings in the axial direction; the inside and outside of the windings are the vertical insulation paper tubes. Meanwhile, a baffle for oil is set up at intervals of a certain number of discs, so as to lead the oil flow in the vertical direction to the horizontal direction, which can enhance the cooling effect of windings. According to the structure characteristic of iron reactor, the influence of iron column and iron yoke on the heat dissipation of windings can be ignored; thus, the windings of iron reactor are only considered in this paper, and the basic structure of windings is given in Figure 1.

2.2. The Equivalent Model of Windings. The total windings consist of 60 layers of disc, and they were divided into 4 channels by the oil guiding washer. Each channel consists of 15 layers of disc, each layer of disc consists of 23 turns of conductor with insulating layers, and the thickness of the insulating layer is 0.4 mm. Considering the temperature and fluid velocity distribution in each channel of the windings are basically the same, thus, one of the channels is selected to research the temperature distribution of windings, and the equivalent model and parameters are given in Figure 2.

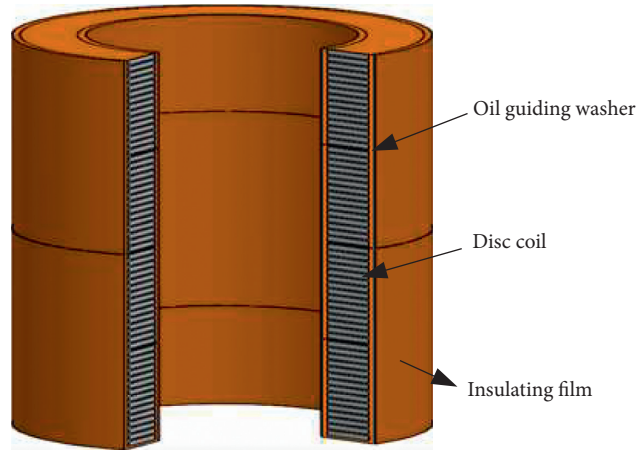

Figure 1: The basic structure of windings.

The characteristics of metal conductor and insulating materials are given in Table 1.

3. The Temperature Calculation of Windings Based on the Thermal Network Model

3.1. The Establishment of Thermal Network Model. The heat transfer model of windings can be equivalent to the circuit node network, which adopts the analogy method between the circuit and the heat transfer system. The basic idea of thermo-electric analogy is to compare the transfer of heat between media to the transfer of electric current in a conductor. The related physical essence of the temperature field is analogized to the heat transfer parameters, such as temperature difference, heat flux, heat resistance, and heat capacity. So, the topology of the thermal network can be established, and it is similar to the circuit [22]. In order to obtain the temperature distribution of each conductor and oil flow node, a thermal network model with each conductor as the basic unit is established based on the equivalent model of windings, as shown in Figure 3.

In Figure 3, T_{disc} and T_{oil} are the node temperature of conductor and oil flow, respectively, R_{cir} is the conduction thermal resistance between conductors and insulating layers, R_{oor} is the conduction thermal resistance of oil flow, R_{ior} is the convection thermal resistance between the insulation layers and oil, and q is the heat source of the conductor.

3.2. The Calculation of Thermal Resistance. In the actual operation process of oil-immersed iron core reactor, the influence of the leakage magnetic on the eddy current loss of each turn is basically the same, so it is considered that each turn conductor has the same heat source. Considering the temperature difference between the adjacent conductors is

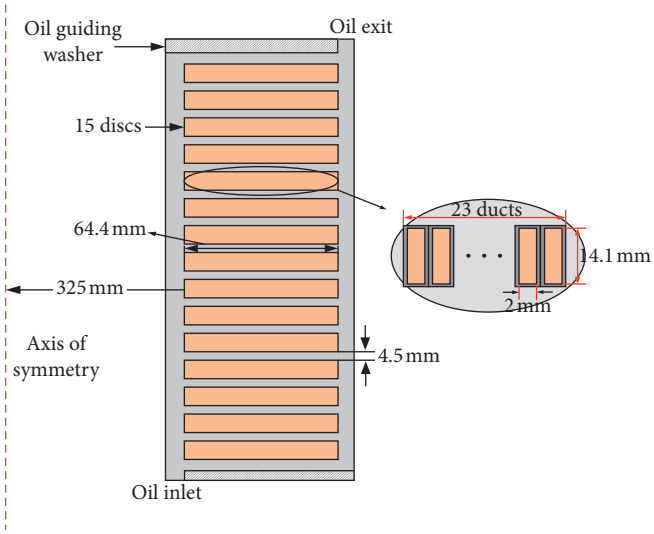

Figure 2: The equivalent model of windings.

Table 1: The characteristics of metal conductor and insulating materials.

Materials	Attribute	Value
Copper	Heat conductivity ($W \cdot M^{-1} \cdot K^{-1}$)	400
	Specific heat ($W \cdot kg^{-1} \cdot K^{-1}$)	385
	Density ($Kg\ M^{-3}$)	8940
Insulating materials	Heat conductivity ($W \cdot M^{-1} \cdot K^{-1}$)	0.21
	Specific heat ($W \cdot kg^{-1} \cdot K^{-1}$)	1250
	Density ($Kg\ M^{-3}$)	870

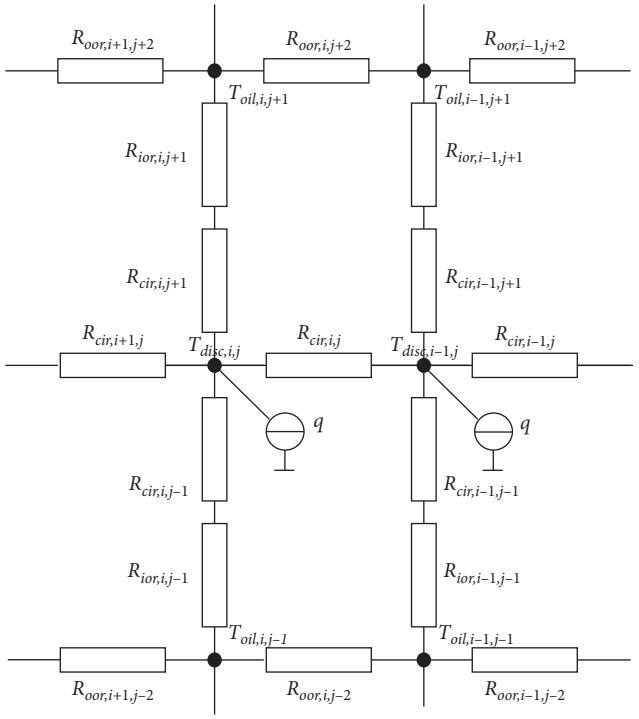

Figure 3: The thermal network model.

small, the radiation heat transfer can be ignored, so the heat transfer modes of heat flux in the four directions of the conductor are merely the heat conduction and heat convection. In order to establish the thermal network model, the calculation of thermal resistance is essential.

(1) The conduction thermal resistance: in the inner of conductors and insulating material, the conduction thermal resistance depends on the geometric structure and material properties. When the heat flux is transferred to the oil channel, the heat transfer will occur in the oil flow, and the conduction thermal resistance of the oil flow is related to the geometric shape of the oil channel and physical properties of the oil. The conduction thermal resistance in the conductors, insulation layers and oil can be calculated, as shown in the following equation:

$$R_{(\mathrm{cir/oor})} = \frac{L_q}{k_m S}, \tag{1}$$

where L_q is the thickness of the conductor in the direction in which the heat flows, k_m is the thermal conductivity of material, S is the surface area, which is perpendicular to heat flow direction, R_{cir} is the conduction thermal resistance of metal conductor and insulating layers, and R_{oor} is the conduction thermal resistance of oil.

(2) The convection thermal resistance: the convection heat transfer is formed between the discs and the horizontal and vertical oil channel, and the thermal resistance is related to the fluid velocity and temperature of oil. According to the Newton's law of cooling, the convection thermal resistance between the surfaces of the insulating layers and the oil channels can be expressed, as shown in the following equation:

$$R_{\mathrm{ior}} = \frac{1}{\alpha A}, \tag{2}$$

where R_{ior} is the convection thermal resistance between the insulation layers and oil, A is the area of the insulating layer, and α is the convection coefficient, which is related to the geometric structure, material, and fluid characteristics of oil, and it can be written as follows:

$$\alpha = \frac{N_u k_{\mathrm{oil}}}{L_{io}}, \tag{3}$$

where L_{io} is the geometric characteristic length of the convection heat transfer surface, k_{oil} is the thermal conductivity of transformer oil, and N_u is the Nusselt number, and the expression is [23]

$$N_u = 1.86\left(\frac{R_e P_r D}{L}\right)^{(1/3)}\left(\frac{\mu}{\mu_s}\right)^{0.14}, \tag{4}$$

where L is the horizontal length, D is the diameter of oil channel, μ is the kinetic viscosity of oil with the ambient temperatures, μ_s is the kinetic viscosity of

oil, R_e is the Reynolds number, and P_r is the Prandtl number. The parameters, R_e and P_r, can be calculated by the following equation:

$$\begin{cases} R_e = \dfrac{\rho_{\text{oil}} v_i D}{\mu_s}, \\ P_r = \dfrac{c_p \mu_s}{k_{\text{oil}}}, \end{cases} \tag{5}$$

where ρ_{oil} and c_p are the density and specific heat capacity of oil, respectively, and v_i is the fluid velocity of horizontal oil channel in the i_{th} layer.

3.3. The Temperature Calculation of Windings. According to the thermal network model in Figure 3, it contains N nodes, so the n-1 node equations can be listed [21], which is similar to the node voltage equation in the circuit. The temperature equations of each node can be written [24], as shown in the following equation:

$$\begin{cases} \left(\sum \dfrac{1}{R_{\text{self-impedance}}}\right) T_{\text{disc},i,j} - \sum\left(\dfrac{1}{R_{\text{mutual-impedance}}} T_{\text{disc},m_i,j}\right) - \sum\left(\dfrac{1}{R_{\text{mutual-impedance}}} T_{\text{oil},i,n_j}\right) = q, \\ \left(\sum \dfrac{1}{R_{\text{self-impedance}}}\right) T_{\text{oil},i,j} - \sum\left(\dfrac{1}{R_{\text{mutual-impedance}}} T_{\text{disc},m_i,j}\right) - \sum\left(\dfrac{1}{R_{\text{mutual-impedance}}} T_{\text{oil},i,n_j}\right) = 0, \end{cases} \tag{6}$$

where $R_{\text{self-impedance}}$ is the node self-thermal resistance, $R_{\text{mutual-impedance}}$ is the node mutual thermal resistance, $T_{\text{disc},i,j}$ and $T_{oil,i,j}$ are the conductor and oil flow nodes of the *ith* row and *jth* column in the model, respectively, m_i and n_j are the numbers of adjacent nodes, $m_i = (i-1, i+1)$, $n_j = (j-1, j+1)$. The above equation can be solved by the MATLAB software, and the node temperature can be expressed as

$$T = G^{-1} Q, \tag{7}$$

where T is the temperature of node, Q is the heat source matrix of the conductor, and G is the heat conductivity matrix, which is composed by the self-thermal resistance and mutual thermal resistance, as shown in the following equation:

$$G = \begin{bmatrix} \dfrac{1}{R_{sa\_1}} & -\dfrac{1}{R_{ma1\_1}} & 0 & \cdot & -\dfrac{1}{R_{ma2\_1}} & \cdot & 0 & 0 \\ -\dfrac{1}{R_{ma1\_1}} & \dfrac{1}{R_{sa\_2}} & -\dfrac{1}{R_{ma1\_2}} & 0 & \cdot & \cdot & \cdot & 0 \\ 0 & -\dfrac{1}{R_{ma1\_2}} & \dfrac{1}{R_{sa\_2}} & -\dfrac{1}{R_{ma1\_3}} & \cdot & \cdot & \cdot & \cdot \\ \cdot & 0 & -\dfrac{1}{R_{ma1\_3}} & \cdot & \cdot & \cdot & \cdot & -\dfrac{1}{R_{ma2\_t}} \\ -\dfrac{1}{R_{ma2\_1}} & \cdot & \cdot & \cdot & \cdot & \cdot & 0 & \cdot \\ \cdot & \cdot & \cdot & \cdot & \cdot & \dfrac{1}{R_{sa\_n-2}} & -\dfrac{1}{R_{ma1\_n-1}} & 0 \\ 0 & \cdot & \cdot & \cdot & 0 & -\dfrac{1}{R_{ma1\_n-1}} & \dfrac{1}{R_{sa\_n-1}} & -\dfrac{1}{R_{ma1\_n}} \\ 0 & 0 & \cdot & -\dfrac{1}{R_{ma2\_t}} & \cdot & 0 & -\dfrac{1}{R_{ma1\_n}} & \dfrac{1}{R_{sa\_n}} \end{bmatrix}, \tag{8}$$

where, $(1/R_{ma1\_i})$ and $(1/R_{ma2\_j})$ are the sum of mutual admittance of the ith and jth nodes, respectively, and the parameter, $(1/R_{sa\_i})$, is the sum of self-admittance of the node.

According to the structure and electrical parameters of windings, combined with the above calculation method, the temperature of each node can be obtained by solving equation (7).

3.4. The Calculation Results Based on Thermal Network Model. The settings of thermal network model are as follows: the loss of each turn conductor is 34.5 W, the temperature in the inlet of the oil channel is 303.15 K, and the velocity is 0.3 m/s; the boundary conditions of the upper and lower surfaces of each channel are heat insulation as the low thermal conductivity of the oil guide baffle. In the thermal network model, there exist 437 conductor nodes and 460 oil channel nodes; the number of the discs is sorted from top to bottom; combined with the thermal resistance calculation method and node temperature equation, the temperature of each node can be obtained, and the maximum temperature of each disc is given, as shown in Table 2.

In Table 2, it can be seen that the maximum temperature of discs is gradually increased from the bottom to the top, but there is a downward trend when nearing the top, the maximum temperature is 62.65°C, and the maximum temperature area is mainly concentrated in the upper middle position of winding; the main reason is that the fluid velocity of oil is large in the inlet and outlet, and the convection heat transfer degree is high. When the oil flows in the long channel, the temperature is increased and the fluid velocity of oil is decreased, which leads to the accumulation of heat in the middle of windings, so the temperature of the middle discs is higher than the upper and lower discs.

4. Model Validation

4.1. The Finite Element Simulation Calculation. According to the structure parameters and material characteristics of the windings, the two-dimensional model is established based on the COMSOL, as shown in Figure 4.

The governing equations and boundary conditions settings are the key steps of simulation calculation.

4.1.1. Governing Equation. The heat conduction and heat convection are the main heat transfer processes in the windings region, and the governing equation of heat conduction can be expressed by the following equation [25]:

$$\frac{\partial^2 T}{\partial r^2} + \frac{\partial^2 T}{\partial z^2} + \frac{q}{k_m} = 0. \tag{9}$$

The heat convection between windings and oil channels satisfies mass, momentum, and energy conservation, as shown in the following equation [26]:

$$\begin{cases} \dfrac{1}{r}\dfrac{\partial (ur)}{\partial r} + \dfrac{1}{z}\dfrac{\partial (vr)}{\partial z} = 0, \\ \rho_{\text{oil}}\left(u\dfrac{\partial u}{\partial r} + v\dfrac{\partial u}{\partial z}\right) = F_r - \dfrac{\partial p}{\partial r} + \mu_s\left(\dfrac{\partial^2 u}{\partial r^2} + \dfrac{\partial^2 u}{\partial z^2}\right), \\ \rho_{\text{oil}}\left(u\dfrac{\partial v}{\partial r} + v\dfrac{\partial v}{\partial z}\right) = F_z - \dfrac{\partial p}{\partial z} + \mu_s\left(\dfrac{\partial^2 v}{\partial r^2} + \dfrac{\partial^2 v}{\partial z^2}\right), \\ u\dfrac{\partial T}{\partial r} + v\dfrac{\partial T}{\partial z} = \dfrac{k_{\text{oil}}}{\rho_{\text{oil}} c_p}\left(\dfrac{\partial^2 v}{\partial r^2} + \dfrac{\partial^2 v}{\partial z^2}\right), \end{cases} \tag{10}$$

where u and v are the radial and axial fluid velocities of oil, respectively, F_r and F_z are the radial and axial components of fluid gravity, and p is the pressure of fluid.

4.1.2. The Boundary Conditions Setting. The boundary conditions are set as follows: (1) the heat transfer between the insulating paper and the outer transformer oil can be ignored, and it sets as an adiabatic boundary. (2) The discs surface is regarded as the stationary, the axial and radial velocity are zero, the inlet velocity of oil is 0.3 m/s, and the temperature is 303.15 K. (3) The outlet boundary condition of oil flow is natural pressure outlet boundary and the axis of rotation is axisymmetric boundary condition. The heat source of each turn conductor is setting the same; the value is 34.5 W. Meanwhile, the characteristic parameters of oil are given in Table 3.

4.2. The Simulation Results. The transient field is applied in the simulation, the total calculation time is 10 h, and the time step is 0.1 h, which can be considered that it has reached the steady state. The temperature of windings and fluid velocity distribution of oil are given in Figure 5.

In Figure 5, the temperature of discs in the inlet is lower than in the middle, and the maximum temperature reaches 66.20°C in the 8th disc; the fluid velocity of oil is relatively large in the inlet and outlet. In order to analyze the heat transfer process of discs, the radial and axial direction paths are extracted, as shown in Figure 6.

According to the paths selected and simulation results, the temperature distribution with the different paths is plotted, as shown in Figures 7–9.

From Figures 7–9, it can be seen that the temperature of discs is increased first and then decreased in axial and radial directions. On the contrary, the fluid velocity along the axial direction is decreased first and then increased, which is opposite to the trends of temperature. Meanwhile, the maximum temperature locates the eighth disc, and the fluid velocity is the lowest on the both sides of the discs with the maximum temperature, the main reasons are that the fluid velocity in lower channels is relatively large when the oil passes the inlet, and the temperature is low. The heat

Table 2: The maximum temperature of each disc.

Disc number	1	2	3	4	5	6	7	8
Temperature (℃)	40.79	45.58	50.47	55.49	59.33	61.35	62.32	62.65
Disc number	9	10	11	12	13	14	15	
Temperature (℃)	62.56	62.17	61.54	60.73	59.77	58.68	57.47	

dissipation conditions are weak because of the high temperature and low velocity of the oil in the middle discs; the temperature of the middle discs is the highest. In the upper discs, the oil converges in the outlet; it leads to the increase of the fluid velocity, so the temperature of the upper discs is lower compared with the middle discs.

4.3. Model Validation. In order to verify the accuracy of the thermal network model, the maximum temperature of each disc is obtained in both the thermal network model and finite element method, as shown in Figure 10.

In Figure 10, it can be seen that the maximum temperature is basically the same based on the thermal network model and finite element method, and the maximum error coefficient of the disc is only 5.30%, which locates the 8th disc, so the correctness of the thermal network model is verified.

The error coefficient is defined as follows:

$$\varepsilon = \left| \frac{T_{\text{hot}} - T_{\text{COM}}}{T_{\text{COM}}} \right|, \tag{11}$$

where ε is the error coefficient, T_{hot} is the temperature based on the thermal network model, and T_{COM} is the temperature based on the finite element method. Meanwhile, the thermal network model is a multivariate linear equation related to thermal resistance, and the calculation speed is fast compared with the finite element method; thus, the thermal network model is adopted to optimize the windings in this paper.

5. The Optimization Design of Windings Based on Particle Swarm Algorithm and Thermal Network Model

According to actual engineering requirements of the oil-immersed iron core reactor, the metal conductor usage and loss of windings are the two major optimization objects; however, these goals are in conflict with each other, the performance improvement of one object results in the reduction of the other object. In order to achieve the optimal design parameters of windings, the optimization design of iron reactor is needed.

5.1. The Particle Swarm Optimization Algorithm. The particle swarm optimization is one of the most influential multiobjective algorithms, including the prominent characteristics: the optimal solution of multiobjective can be easily obtained for its efficient search ability, and the algorithm has good multipeak search ability, which means it has a good ability to search for a global optimal value and it converges quickly. The flow chart of particle swarm optimization method is given in Figure 11.

The formulas of particle update in particle swarm optimization are as follows [27]:

$$\begin{aligned} V^{k+1} &= wV^k + c_1 r_1 \left(P_i^k - X^k\right) + c_2 r_2 \left(P_g^k - X^k\right), \\ X^{k+1} &= X^k + V^{k+1}, \end{aligned} \tag{12}$$

where w is the inertia weight, r_1, r_2 are the random numbers distributed in [0, 1], k is the current iteration number, P_i is the individual optimal particle position, P_g is the global particle position, c_1, c_2 are the acceleration constants, V is the velocity of the particle, and X is the position of the particle.

The optimization object is to obtain the minimum metal conductor usage and loss of windings; according to the structural characteristics of the windings, the size of the conductor W_{coil}, the height of horizontal channels H_{coil}, and the thickness of insulation layer L_{ins} are selected as the optimization variables. The object functions of metal conductor usage M_{cu} and loss P_{loss} can be written as

$$\begin{cases} \min M_{\text{cu}} = \pi \rho m \displaystyle\sum_{i=1}^{n_{\text{disc}}} d_i W_{\text{coil}} H_{\text{coil}}, \\ \min P_{\text{loss}} = \pi I^2 \gamma \displaystyle\sum_{i=1}^{n_{\text{disc}}} \frac{d_i}{W_{\text{coil}} H_{\text{coil}}}, \end{cases} \tag{13}$$

where ρ is the density of metal conductor, m is the number of discs, n_{disc} is the number of conductors in each disc, d_i is the average diameter of the i_{th} conductor, I is the current of the conductor, and γ is the resistance of the conductor.

The inequality constraints are

$$\begin{cases} T_{\text{Hot\_max}} \le T_{\max}, \\ L_{\min} \le L \le L_{\max}, \\ W_{\text{coil\_min}} \le W_{\text{coil}} \le W_{\text{coil\_max}}, \\ H_{\text{coil\_min}} \le H_{\text{coil}} \le H_{\text{coil\_max}}, \\ H_{\text{duct\_min}} \le H_{\text{duct}} \le H_{\text{duct\_max}}, \end{cases} \tag{14}$$

where $T_{\text{Hot\_max}}$ is the maximum temperature of discs by calculation methods, $T_{\max}$ is the maximum temperature constraints of the discs, L is the inductance of the reactor, and $W_{\text{coil\_min}}$, $W_{\text{coil\_max}}$, $H_{\text{coil\_min}}$, $H_{\text{coil\_max}}$, $H_{\text{duct\_min}}$, and $H_{\text{duct\_max}}$ are the minimum and the maximum values of variables.

5.2. The Optimization Results. In particle swarm optimization algorithm, the variable parameters are set as follows: the radial width of the conductor is [1.6, 2.6] mm, the axial

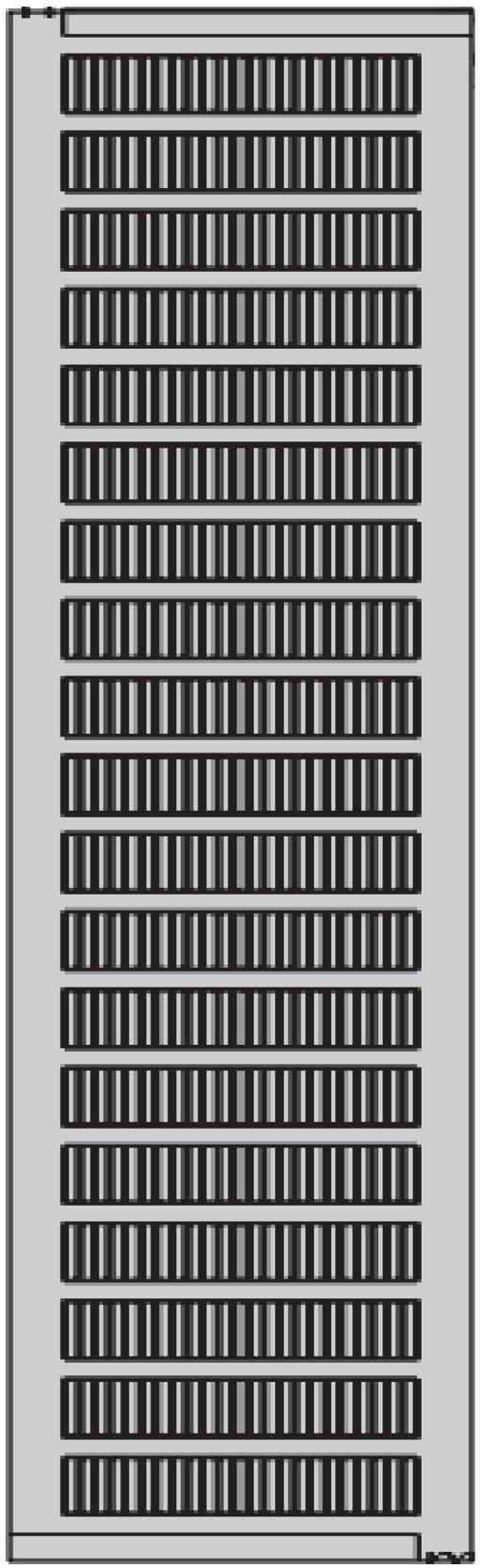

Figure 4: The simulation model of windings.

Table 3: The characteristics of oil.

Materials	Attribute	Value
Oil	Heat conductivity ($W \cdot M^{-1} \cdot K^{-1}$)	$0.134 - 8.05 \times 10 - 5T$
	Specific heat ($W \cdot kg^{-1} \cdot K^{-1}$)	$-13408.15 + 123.04T - 0.33T\hat{}2$
	Density ($Kg\ M^{-3}$)	$1055.05 - 0.58T - 6.4 \times 10 - 5T\hat{}2$
	Dynamic viscosity ($kg \cdot M^{-1} \cdot S^{-1}$)	$91.45 - 1.33T + 0.01T\hat{}2$

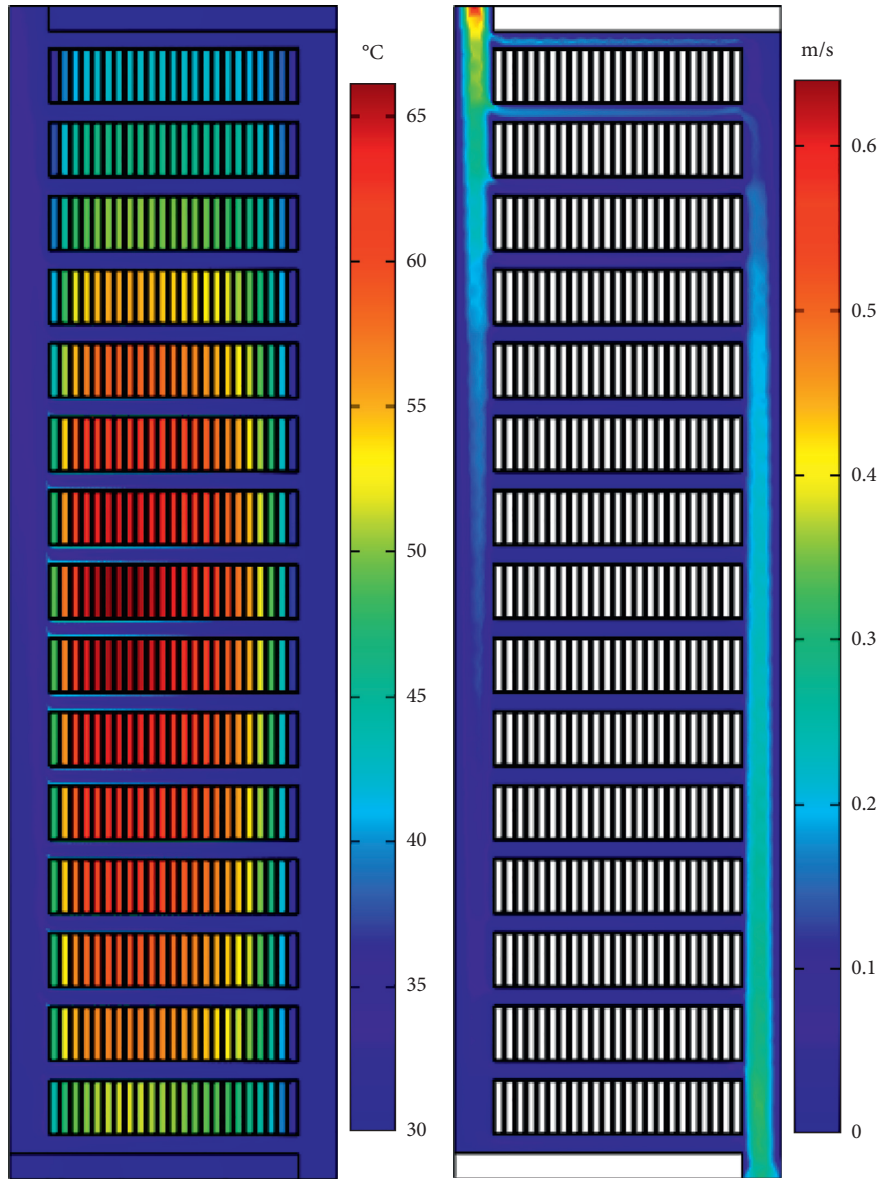

Figure 5: Simulation results: (a) temperature distribution; (b) fluid velocity distribution.

height of the conductor is [12, 14.6] mm, the thickness of the insulation layer is [0.25, 0.5] mm, and the height of horizontal channels is [3.9, 5.4] mm. The expected inductance difference is less than 2%, and the maximum temperature of winding is 75°C. The settings of particles in particle swarm optimization are as follows: the acceleration constants c_1 and c_2 are 0.8, the iteration time is 200, and the inertia weight value is 0.8–1.2. The Pareto optimum results are shown in Figure 12,

The change rate of metal conductor usage and loss, K_M and K_{loss}, is defined as the following equation:

$$K_x = \frac{x}{x_0}, \tag{15}$$

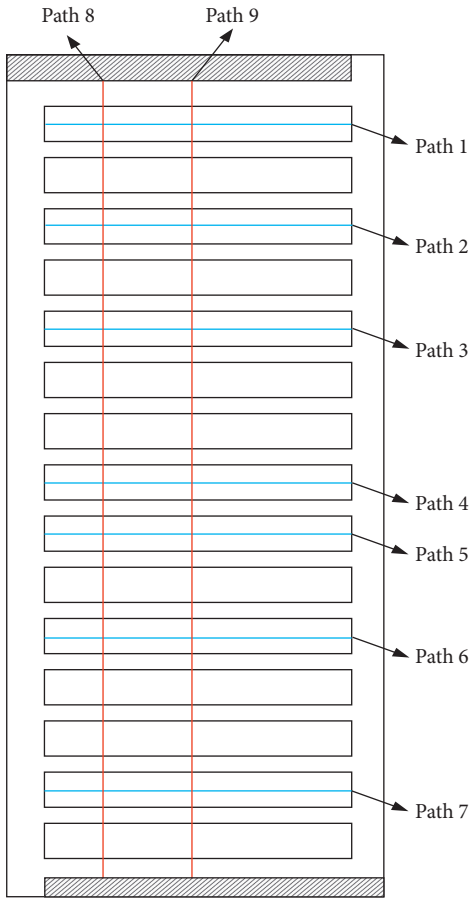

Figure 6: The extract path of the model.

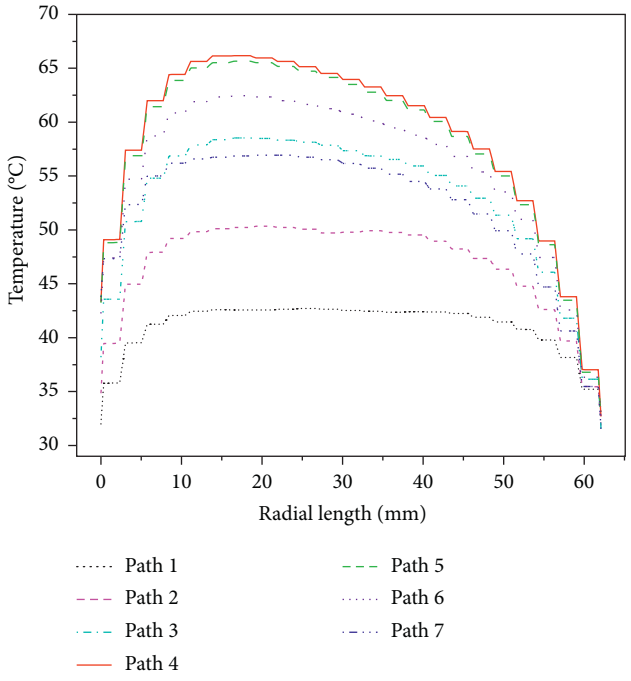

Figure 7: The temperature rise distribution along the radial paths.

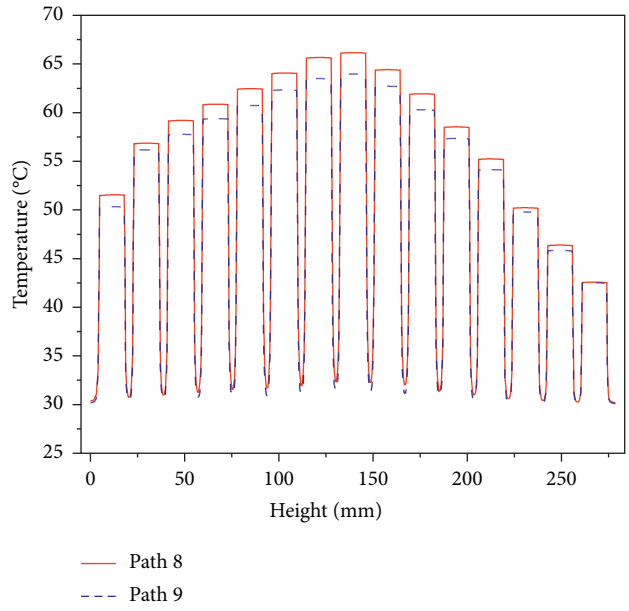

Figure 8: The temperature rise distribution along the axial paths.

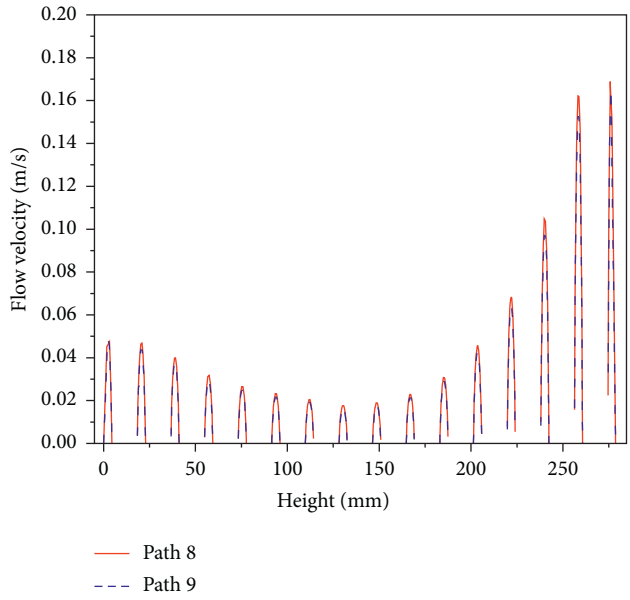

Figure 9: The fluid velocity distribution along the horizontal paths.

where x_0 is the initial design parameter and x is the design parameter with the optimization method. In the initial parameters, the metal conductor usage and loss of windings are 90.98 kg and 11.9 kW before optimization, respectively.

In Figure 12, it can be seen that there exists an opposite trend between the metal conductor usage and loss of windings. Combined with the particle swarm optimization algorithm and thermal network model, the representative results can be obtained, as shown in Table 4. The inductance change rate is less than 1% compared with the initial parameters.

In order to verify the correctness of the optimization results, taking the groups 2, 9, 17, and 20 in Table 4 as an example, the maximum temperatures of windings are 54.91°C, 67.74°C, 68.56°C, and 73.40°C, respectively, based on the thermal network model. Meanwhile, the simulation results based on the finite element method are given in Figure 13; the maximum temperatures of windings are 55.10°C, 68.20°C, 70.00°C, and 72.63°C respectively; it can be seen that the temperature distribution laws of the four groups are basically the same, and the error coefficient is less than 3%; thus, the correctness of the optimization method has been verified.

In Table 4, it can be seen that the metal conductor usage of windings is reduced by 23.05%, and the loss of the windings is reduced by 20.25% compared with the initial design parameters. As the purpose of low metal conductor

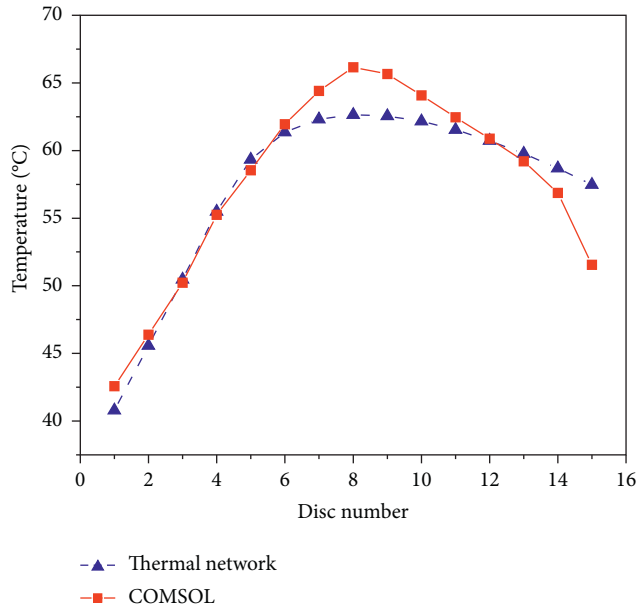

Figure 10: The maximum temperature of each disc.

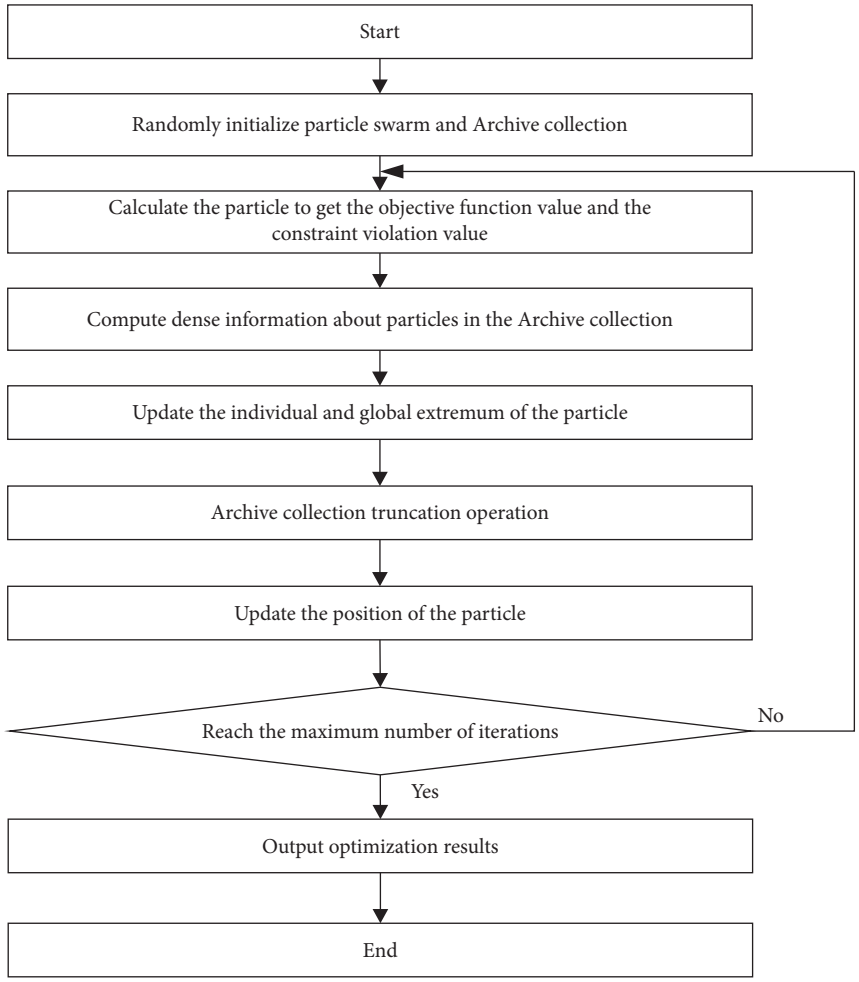

Figure 11: The flow chart of particle swarm optimization algorithm.

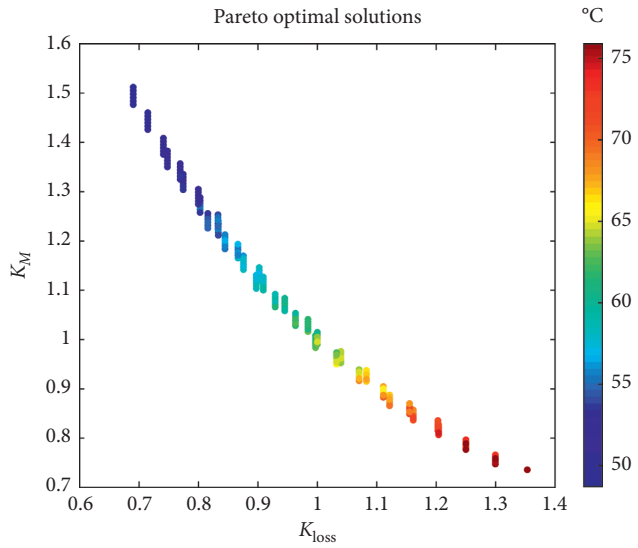

Figure 12: Pareto Frontier of particle swarm optimization.

Table 4: The pareto optimum solutions.

Case	Wcoil (mm)	Hcoil (mm)	Lins (mm)	Hduct (mm)	Loss (kW)	Weight (kg)
1	1.6	13.6	0.35	4.5	15.04	75.57
2	2.6	12.1	0.40	5.1	11.06	109.25
3	1.6	13.1	0.45	4.5	15.61	74.45
4	1.8	12.1	0.45	4.8	15.21	75.64
5	2.4	14.6	0.40	4.2	9.81	121.68
6	1.6	14.1	0.50	3.9	14.51	78.34
7	1.8	13.6	0.40	3.9	13.54	85.01
8	1.8	13.1	0.35	4.8	14.05	81.89
9	1.8	12.6	0.35	3.9	14.61	78.76
10	1.8	13.1	0.50	4.2	14.05	81.89
11	1.6	12.6	0.50	4.2	16.23	70.01
12	2.0	12.1	0.50	4.2	13.87	84.04
13	2.4	13.1	0.40	4.2	10.94	109.18
14	2.6	14.1	0.25	4.2	9.49	127.31
15	1.8	13.1	0.50	4.5	14.06	81.89
16	2.4	14.6	0.40	3.9	9.81	121.68
17	1.8	12.6	0.35	4.2	14.61	78.76
18	2.0	12.1	0.25	5.1	13.86	84.04
19	2.0	12.6	0.30	5.1	13.32	78.75
20	1.6	13.1	0.30	3.9	15.61	72.79

usage and loss of winding are conflicted and cannot be optimized simultaneously, therefore, in the actual design process of the iron reactor, it is necessary to select the suitable structural parameter to realize the optimization of one objective with the other objectives which are not deteriorating.

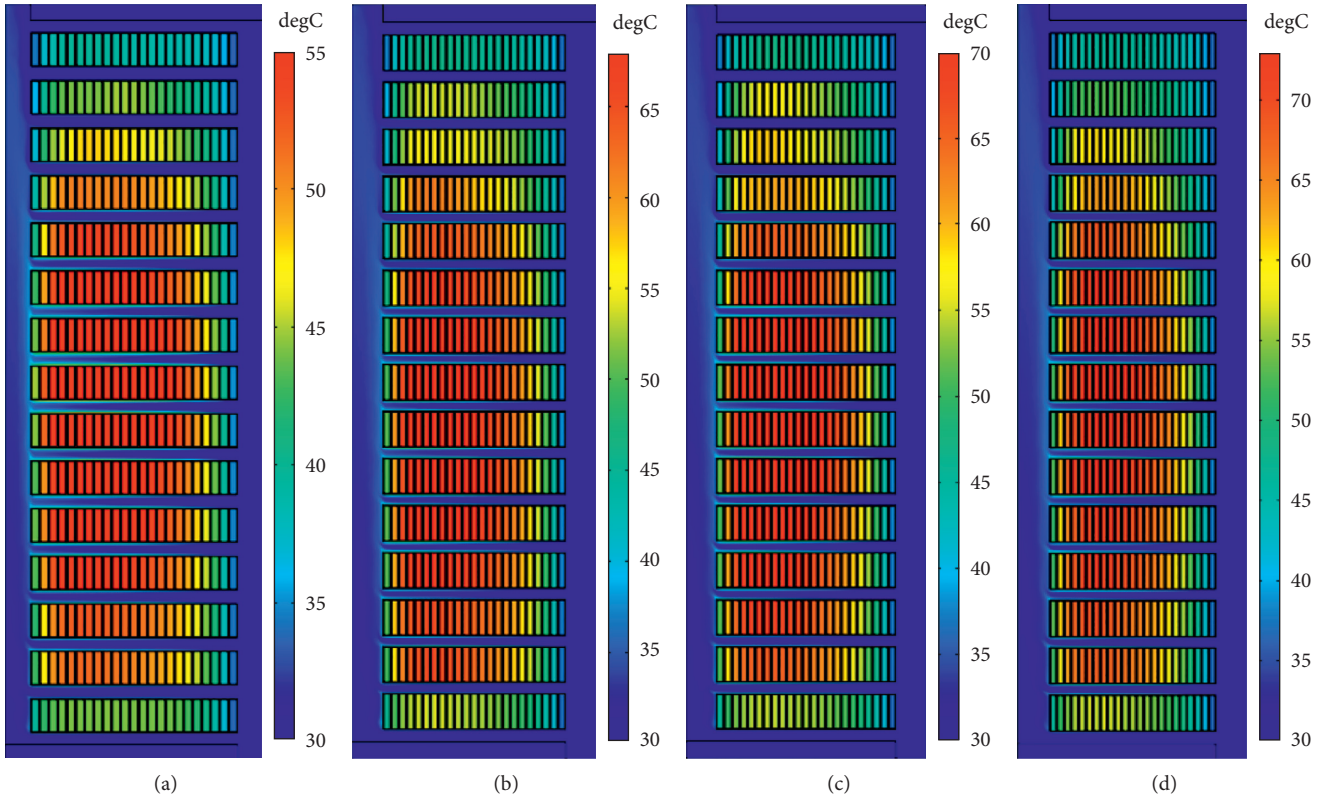

Figure 13: Simulation results: (a) Case 2; (b) Case 9; (c) Case 17; (d) Case 20.

6. Conclusions

According to the structure and parameters of oil-immersed iron core reactor, a multiobjective optimization method based on particle swarm optimization and thermal network model is proposed, and the following conclusions can be obtained:

(1) The maximum temperature error of discs is less than 3% between the thermal network model and finite element method, and the position of the temperature is basically the same; the correctness of thermal network model has been verified

(2) The maximum temperature region is mainly concentration of the middle of windings; the reasons are given by analyzing the fluid velocity distribution of oil, so this area is the main focus to monitoring temperature for the windings

(3) The optimization design of windings based on particle swarm algorithm and thermal network model is proposed, the metal conductor usage is decreased by 23.05%, and the loss of the windings is reduced by 20.25% compared with the initial design parameters, so the optimization method has an important guiding significance for the design of oil-immersed iron core

Data Availability

The data used to support the findings of this study are included in this paper and available without any restriction.

Conflicts of Interest

The authors declare no conflicts of interest.

Acknowledgments

This work was supported by the Natural Science Foundation of Hubei Province (no. 2020CFB376), Hubei Provincial Engineering Technology Research Center for Power Transmission Line Open Fund Project, China Three Gorges University (no. 2019KXL09), and National Natural Science Foundation of China (no. 51977121).

References

[1] H. Yuzhu, *Design Optimization and Multi Physical Field Analysis of Oil Immersed Series Iron-Core Reactor*, Harbin University of Science and Technology, Harbin, China, 2018.

[2] Y. Fating, Y. Zhao, L. Junxiang, W. Yong, and H. Junjia, "Research on temperature field simulation of dry type Air core reactor," in *Proccedings of International Conference on Electrical Machines and Systems Sydney*, IEEE, Australia, August 2017.

[3] X. Tianwei, C. Yundong, J. Wei, and G. Yuanzhi, "The analysis of temperature field in dry air core reactor," *High Voltage Engineering*, vol. 25, no. 4, pp. 86–88, 1999.

[4] D. Qiu, *The Research on Thermal Field Calculation of Tightly Coupled Dry Type Air-Core Split Reactor*, Huazhong University of Science and Technology, Wuhan, China, 2011.

[5] Y. Fating, T. Bo, D. Can, Q. Shihong, H. Li, and Y. Zhao, "Optimization design of a high-coupling split reactor in a

parallel-type circuit breaker," *IEEE Access*, vol. 7, pp. 33473–33480, 2019.

[6] C. Rong, S. W. Yang, and Q. Q. Yan, "Electromagnetic-fluid-temperature coupling calculation and analysis of dry type Air-core shunt reactor," *High Voltage Engineering*, vol. 43, no. 9, pp. 3021–3028, 2017.

[7] J. Zhipeng, W. Xishan, W. Yu, C. Ruizhen, C. Jifeng, and C. Tuteng, "Test and coupling calculation of temperature field for UHV dry type Air-core smoothing reactor," *Proceedings of the CSEE*, vol. 35, no. 20, pp. 5344–5350, 2015.

[8] A. J. Oliver, "Estimation of transformer winding temperatures and coolant flows using a general network method," *IEE Proceedings C Generation, Transmission and Distribution*, vol. 127, no. 6, pp. 395–405, 1980.

[9] C. Joris, V. Wim, and B. Martine, "Assessment of a hydraulic network model for zig zag cooled power transformer windings," *Applied Thermal Engineering*, vol. 80, pp. 220–228, 2015.

[10] A. Weinlader, W. Wu, S. Tenbohlen et al., "Prediction of the oil flow distribution in oil-immersed transformer windings by network modelling and computational fluid dynamics," *IET Electric PowerApplications*, vol. 6, no. 2, pp. 82–90, 2012.

[11] Z. Xiang, W. Zhongdong, and L. Qiang, "Prediction of pressure drop and FlowDistribution in disc type transformer windings in an OD cooling mode," *IEEE Transactions on Power Delivery*, vol. 32, no. 4, pp. 1655–1664, 2017.

[12] Z. Jiahui and L. Xianguo, "Coolant flow distribution and pressure loss in ONAN transformer windings-Part II:optimization of design parameters," *IEEE Transactions on Power Delivery*, vol. 19, no. 1, pp. 194–199, 2004.

[13] Z. Xiang and W. Zhongdong, "Assessment of hydraulic network models in predicting reverse flows in OD cooled disc type transformer windings," *IEEE Access*, vol. 7, pp. 139249–139257, 2019.

[14] J. Smolka and A. J. Nowak, "Shape optimization of coils and cooling ducts in dry-type transformers using computational fluid dynamics and genetic algorithm," *IEEE Transactions on Magnetics*, vol. 47, no. 6, pp. 1726–1731, 2011.

[15] Y. Zhao, H. Junjia, P. Yuan, Y. Xiaogen, L. Chujun, and C. Sizhe, "Research on electromagnetic efficiency optimization in the design of air-core coils," *International Transactions on Electrical Energy Systems*, vol. 25, no. 5, pp. 789–798, 2015.

[16] Y. Fating, T. Bo, D. Can, Q. Shihong, Y. Zhao, and H. Li, "Optimization designof oil-immersed air core coupling reactor for a 160 kV mechanical direct current CircuitBreaker," *Energies*, vol. 12, no. 6, 2019.

[17] L. Zhigang, G. Yingsan, and W. Jianhua, "Optimum design of dry-type air-core series reactor based on modified adaptive genetic algorithm," *Proceedings of the CSEE*, vol. 23, no. 9, pp. 103–106, 2003.

[18] I. Mohamed, A. Abdelwanis, R. Abaza, and A. Elsehiemy, "Parameter estimation of electric power transformers using coyote optimization algorithm with experimental verification," *IEEE Access*, vol. 8, pp. 50036–50043, 2020.

[19] V. D. Shabnam and H. Hossein, "A diversified multi-objective simulated annealing and genetic algorithm for optimizing a three-phase HTS transformer," *IEEE Transactions on Applied Superconductivity*, vol. 26, no. 2, p. 5500210, 2016.

[20] M. S. Mohammed, R. A. Vural, and R. A. Vural, "NSGA-II+FEM based loss optimization of three-phase transformer," *IEEE Transactions on Industrial Electronics*, vol. 66, no. 9, pp. 7417–7425, 2019.

[21] B. Xia, G. G. Jeong, and C. S. Koh, "Cokriging assisted PSO algorithm and its application to optimal transposition design of power transformer windings for the reduction of circulating current loss," *IEEE Transactions on Magnetics*, vol. 52, no. 3, Article ID 7208604, 2016.

[22] Z. R. Radakovic and M. S. Sorgic, "Basics of detailed thermal-hydraulic model for thermal design of oil power transformers," *IEEE Transactions on Power Delivery*, vol. 19, no. 1, pp. 194–199, 2004.

[23] Y. Zhao and M. S. Sorgic, *Research on Thermal and Magnetic Optimization of Carbon-type Multi-enveloped Core Reactor*, Huazhong University of Science and Technology, Wuhan, China, 2014.

[24] C. Bin, L. Lin, Z. Zhibin, Z. Xiwei, and Z. Pengning, "Precision design method of inductance integrated high frequency transformer with large capacity," *Proceedings of the CSEE*, vol. 38, no. 5, pp. 1356–1368, 2015.

[25] Y. Fangting, Y. Zhao, W. Yong, L. Junxiang, and H. Junjia, "Thermal optimization for nature convection cooling performance of air core reactor with the rain cover," *IEEJ Transactions on Electrical and Electronic Engineering*, 2017.

[26] L. Fenxia, L. Ye, and Y. Yunchang, "Numerical and experimental research of internal temperature field of oil immersed core shunt reactor with ultrahigh voltage," *High Voltage Apparatus*, vol. 53, no. 1, pp. 163–168, 2017.

[27] Z. Chenfen, Z. Yanzhen, Z. Jianlong, and M. Xikui, "A diversity guided modified QPSO algorithm and its application in the optimization design of dry type Air-core reactors," *Proceedings of the CSEE*, vol. 32, no. 18, pp. 108–115, 2012.